

# SEISMIC FRAGILITY CURVES OF LIFELINE NETWORKS BASED ON SUBSET SIMULATION

D. Lee<sup>1</sup>, Z. Wang<sup>2</sup> & J. Song<sup>1</sup>

<sup>1</sup> Seoul National University, Seoul, South Korea, [junhosong@snu.ac.kr](mailto:junhosong@snu.ac.kr)

<sup>2</sup> University of California, Berkeley, California, USA

**Abstract:** *For efficient risk assessment of lifeline systems against earthquakes, various empirical and analytical methods have been developed to evaluate the seismic fragility curves of individual structures. However, network reliability, such as origin-destination connectivity after an earthquake, can be more critical for community-level safety. Therefore, beyond the fragility curves of structures, this study proposes a variance reduction sampling framework for fragility curves of network connectivity based on subset simulation. Network reliability analysis faces inherent challenges from complex network topologies, interdependencies among seismic uncertainties, and low-probability network failures. Although various sampling methods, including the crude Monte Carlo simulation (MCS), have been adopted with high flexibility and scalability, they are highly inefficient for sparse network failure events. To overcome this limitation, we reformulate the binary limit-state function used for network connectivity analysis into more informative continuous limit-state functions. The proposed limit-state functions quantify how close each sample is to a network failure, thereby facilitating the construction of intermediate relaxed failure events. A single implementation of Hamiltonian Monte Carlo-based subset simulation (HMC-SS) can generate the network fragility curve by configuring each intermediate failure domain as a network failure event under a given earthquake intensity. A numerical example demonstrates that the proposed framework can accurately and efficiently evaluate network fragility curves.*

## 1 Introduction

Lifeline networks, such as transportation, gas, and electricity systems, are the critical backbone of modern society. Their significance is particularly noticeable in the post-hazard stage because emergency assessment, evacuation, lifesaving, and repair operations rely on lifeline networks' functionality. Therefore, it is essential to assess the network reliability to construct and maintain resilient lifeline networks against seismic hazards. To this end, this study aims to develop an efficient sampling method to assess not only the seismic reliability in terms of two-terminal reliability, but also the network fragility under various earthquake magnitudes.

In large-scale networks, network reliability analysis can be computationally challenging or even infeasible due to the high computation cost, intricate network topology, or interdependencies between components. To reduce the computational challenge known as "combinatorial explosion," various simulation-based approaches, including the crude Monte Carlo simulation (MCS), are extensively used owing to their broad applicability and flexibility. However, the crude MCS has a slow convergence rate of  $\mathcal{O}(N^{-1/2})$ , where  $N$  is the number of random sample points. This slow convergence rate may lead to a prohibitive computation cost in rare event simulations, such as the failures of lifeline networks. To accelerate the probability estimation by sampling in critical regions with higher probabilities, one can introduce subset simulation (SS, Au & Beck 2001), which

relaxes the target failure event into nested intermediate failure events, effectively estimating low probabilities with relatively small samples. An essential ingredient of SS is ranking sample points according to their limit-state function values so intermediate failure events can be formulated.

However, most network limit-state functions in network reliability analyses have binary or multi-state outputs. This feature poses significant challenges for SS because the sample points outside the failure domain have the same limit-state function value; consequently, the algorithm cannot move toward the failure domain as there is no information to guide the sampling in the correct direction. To solve this problem, this study proposes piecewise continuous reformulations of the binary limit-state function representing network disconnection. These new limit-state functions enable the construction of relaxed, intermediate failure events, readily usable in SS. Since the reformulations involve trade-offs in accuracy and efficiency, one can select the limit-state function that aligns better with the analysis goals. Another main contribution of this paper is an alternative interpretation of the intermediate failure domains in the context of subset simulation-based network fragility analysis. By discovering an implicit connection between intermediate failure events and earthquake magnitude, a single simulation of SS can generate the entire network fragility curve.

The paper is organized as follows. Section 2 provides an overview of the seismic network reliability analysis. Section 3 briefly reviews SS, develops informative network limit-state functions, and proposes a computational framework for network fragility analysis. In Section 4, a numerical example demonstrates the performance of the proposed method. Finally, Section 5 summarizes the paper and provides future research directions.

## 2 Seismic network reliability analysis

### 2.1 Failure probabilities of networks components

For seismic network reliability analysis, one should first assess the seismic risk of individual components/structures in a network. The seismic failure of a component is defined as the event that the seismic demand exceeds the seismic capacity, both of which are uncertain. The Bernoulli variable  $B_i$  representing the failure event of component  $i$ , which represents the event when the seismic demand  $D_i$  exceeds the seismic capacity  $C_i$ , is defined as

$$B_i = \mathbb{I}(C_i \leq D_i) = \mathbb{I}(z_i \leq 0), \quad (1)$$

where  $\mathbb{I}(\cdot)$  denotes a binary indicator function that returns 1 if the given inequality holds, and 0 otherwise; and  $z_i = \ln C_i - \ln D_i$  denotes the logarithmic safety margin (Der Kiureghian 2022). The seismic demand  $D_i$  and the seismic capacity  $C_i$  are assumed to be statistically independent, and both are modeled as lognormal distributions. Then,  $z_i$  follows a normal distribution with a mean  $\mu_{z_i} = \ln \bar{C}_i - \ln \bar{D}_i$  and a variance  $\sigma_{z_i}^2 = \zeta_i^2 + \sigma_\eta^2 + \sigma_\varepsilon^2$ , where  $\bar{C}_i$  and  $\bar{D}_i$  are the medians of  $C_i$  and  $D_i$ , respectively,  $\zeta_i$  is the lognormal standard deviation of  $C_i$ , and  $\sigma_\eta$  and  $\sigma_\varepsilon$  are the standard deviations of inter- and intra-event residuals of  $D_i$ , respectively. Then, the joint failure probability of components numbered from 1 to  $N$  is given as

$$P\left(\bigcap_{i=1}^N \{B_i = 1\}\right) = P\left[\bigcap_{i=1}^N \{z_i \leq 0\}\right] = \Phi_N(-\boldsymbol{\beta}, \mathbf{R}_{zz}), \quad (2)$$

where  $\Phi_N(\cdot, \cdot)$  is the  $N$ -variate zero-mean, unit variance normal cumulative distribution function;  $\boldsymbol{\beta} = [\beta_1, \dots, \beta_N]^T$  is the vector of reliability indices, whose component is defined as  $\beta_i = \frac{\mu_{z_i}}{\sigma_{z_i}}$ ;  $\mathbf{R}_{zz} = [\rho_{z_i z_j}]_{i,j \in [1, N]}$  is the  $N \times N$  correlation matrix, which is equivalent to the covariance matrix in the present context; and  $\rho_{z_i z_j}$  is the correlation coefficient between  $z_i$  and  $z_j$ . Lee and Song (2021) analytically derived the correlation coefficient  $\rho_{z_i z_j}$  as

$$\rho_{z_i z_j} = \frac{\zeta_i \zeta_j \delta_{ij} + \sigma_\eta^2 + \sigma_\varepsilon^2 \rho_{\varepsilon_i \varepsilon_j}}{\sqrt{\zeta_i^2 + \sigma_\eta^2 + \sigma_\varepsilon^2} \sqrt{\zeta_j^2 + \sigma_\eta^2 + \sigma_\varepsilon^2}}, \quad (3)$$

where  $\delta_{ij}$  is the Kronecker delta, which is 1 when  $i = j$ , and 0 otherwise; and  $\rho_{\varepsilon_i \varepsilon_j}$  is the correlation coefficients between  $\varepsilon_i$  and  $\varepsilon_j$ .

## 2.2 Network reliability analysis

A lifeline network consists of line-type components, such as pipelines and roads, and node-type components, such as stations and bridges. The network can be described by a graph  $G(\mathbf{V}, \mathbf{E})$ , where  $\mathbf{V}$  denotes the set of nodes (or vertices) representing both types of components, and  $\mathbf{E}$  is the set of links (or edges) indicating the conceptual connectivity between nodes. That is, it is assumed that all links in set  $\mathbf{E}$  are perfectly reliable. This assumption will not cause error in the network reliability analysis because nodes represent the physical entities. The above assumption still holds for networks with link failures to equivalent networks with node failures.

Consider a network state vector  $\mathbf{z} = [z_1, \dots, z_N]$ , denoting a vector of the logarithmic safety margins of components, where  $N = |\mathbf{V}|$  is the number of nodes (i.e., the total number of node-type and line-type components) in the network of interest. The network reliability problem computes the network failure probability  $P_f$  by  $N$ -fold integral in the space of the network state vector, i.e.,

$$P_f = \int_{\mathcal{F}} f_{\mathbf{z}}(\mathbf{z}) d\mathbf{z} = \int_{\mathbb{R}^N} \mathbb{1}(G(\mathbf{z}) \leq 0) f_{\mathbf{z}}(\mathbf{z}) d\mathbf{z}, \quad (4)$$

where  $\mathcal{F} = \{G(\mathbf{z}) \leq 0\}$  is the failure domain for the network reliability problem, such as OD connectivity;  $G(\mathbf{z}) \in \mathbb{R}$  is the network limit-state function; and  $f_{\mathbf{z}}(\mathbf{z})$  is the joint probability density function of the network state vector  $\mathbf{z}$ . For the connectivity between an OD pair, the network limit-state function,  $G_{OD}(\mathbf{z})$ , is defined as the binary limit-state function as

$$G_{OD}^{\text{Bi}}(\mathbf{z}) = \begin{cases} 1, & \text{if the OD pair is connected in } \mathbf{z}, \\ 0, & \text{otherwise,} \end{cases} \quad (5)$$

which depends on the network topology. For example, in a series system, only the joint survival of all components guarantees connectivity. In contrast, a parallel system will fail if and only if all components fail. However, reliability problems for general networks are known to be NP-hard problems (Rosenthal 1977); there is no polynomial-time algorithm to find all component state combinations that express OD connectivity. That is, reliability analyses of large-scale networks often face challenges in (1) exploration of the failure domain in  $2^N$  component state combinations, and (2) fast and accurate computation of probability in the high-dimensional space  $\mathbb{R}^N$ . Therefore, non-simulation-based approaches can be inappropriate for large-scale networks.

## 3 Subset simulation for network reliability analysis

Subset simulation (SS, Au & Beck 2001) is one of the most widely used variance-reduction sampling approaches. In SS, the failure domain of interest,  $\mathcal{F}$ , is represented by  $m$  nested intermediate failure domains,  $\mathcal{F}_1 \supset \mathcal{F}_2 \supset \dots \supset \mathcal{F}_m = \mathcal{F}$ . The failure probability  $P_f$  is expressed as the product of the conditional probabilities  $P(\mathcal{F}_k | \mathcal{F}_{k-1})$ , i.e.,

$$P_f = \prod_{k=1}^m P(\mathcal{F}_k | \mathcal{F}_{k-1}) \cong \frac{p_0^{m-1}}{n} \sum_{j=1}^n \mathbb{1}(\mathbf{z}^{(j)} \in \mathcal{F} | \mathcal{F}_{m-1}), \quad (6)$$

where  $\mathcal{F}_0 = \mathbb{R}^N$  denotes the initial null failure domain. By setting each (except the last) conditional probability identical to a constant  $p_0$ , the intermediate failure domains  $\mathcal{F}_k$ ,  $k = 1, \dots, m-1$ , are adaptively determined by the  $p_0$  quantile of limit-state function values associated with sample points in  $\mathcal{F}_{k-1}$ ;  $n$  is the number of sample points generated in each intermediate failure domain; and  $\mathbf{z}^{(j)}$  is the  $j^{\text{th}}$  sample point. Au and Beck (2001) proposed setting  $p_0 = 0.1$ . While generating independent and identically distributed samples from the initial null failure domain is typically feasible and straightforward, it becomes challenging for the intermediate failure domains  $\mathcal{F}_{k-1}$ ,  $k \geq 2$ . To this end, Markov Chain Monte Carlo (MCMC) methods can be utilized. Using an MCMC method, each conditional probability  $P(\mathcal{F}_k | \mathcal{F}_{k-1})$  and the failure probability estimation  $P_f$  can be calculated.

SS is particularly efficient for rare events because the number of samples required for a single run of SS is  $n_{SS} \propto |\log P_f|$ , while the crude MCS requires  $n_{MCS} \propto 1/P_f$  simulations. MCMC methods have a critical impact on the performance of SS; ideally, the MCMC sample should show limited random walk behavior and achieve rapid mixing. In this work, we adopt the Hamiltonian Monte Carlo-based subset simulation (HMC-SS), an efficient variant of SS leveraging the desirable properties of HMC (Wang et al. 2019).

### 3.1 Informative network limit-state function for subset simulation

The OD connectivity is typically represented by the binary limit-state function in Eq. (5). This property is a major obstacle to using SS in network reliability analysis. Provided with a binary function, the  $p_0$  quantile of the samples is chosen to be either 0 or 1 in each intermediate domain, so SS may not identify the failure domain effectively. To address this problem, the binary network limit-state function  $G_{OD}^{Bi}(\mathbf{z})$  should be reformulated as a multi-state or continuous function. In this study, we propose an informative network limit-state function, which encodes the same failure domain as the original binary function but provides additional information on the direction and distance to the failure domain. To this end, we introduce a path connecting an OD pair. Then, the network limit-state function is defined as follows:

$$G_{OD}^{Pro}(\mathbf{z}) = \begin{cases} \frac{\min_{i \in \mathbf{P}} z_i}{n_p}, & \text{if the OD pair is connected in } \mathbf{z}, \\ 0, & \text{otherwise,} \end{cases} \quad (7)$$

where  $\mathbf{P}$  denotes the set of nodes on the path with positive  $z_i$ ; and  $n_p$  is the number of nodes in  $\mathbf{P}$ . The limit-state function proposed in Eq. (7) stems from the observation that (1) the network survives if there are one more path between the OD pair, and (2) the larger  $n_p$  is, the more likely the path tends to fail. Because of the denominator  $n_p$ , the proposed function is piecewise rather than globally continuous; there may be a discontinuity along the boundaries where  $\mathbf{P}$  changes. To find a path, Dijkstra's algorithm or the breadth-first search (BFS) can be used. Let the  $k^{th}$  intermediate failure domain  $\mathcal{F}_k$  be  $\{G_{OD}^{Pro}(\mathbf{z}) \leq g_k\}$ . Then, according to Eq. (6), the failure probability  $P_f$  is expressed as the product of conditional probabilities as

$$\hat{P}_f \cong \frac{p_0^{m-1}}{n} \sum_{j=1}^n \mathbb{I}(G_{OD}^{Pro}(\mathbf{z}^{(j)}) \leq g_m | G_{OD}^{Pro}(\mathbf{z}^{(j)}) \leq g_{m-1}), \quad (8)$$

where  $g_1 > \dots > g_m = 0$  denote intermediate thresholds;  $g_0 = \infty$  denotes the initial failure threshold; and  $\mathbf{z}^{(j)}$  is the state vector of the components in the  $j^{th}$  network-state sample point. Detailed descriptions on  $G_{OD}^{Pro}$  can be found in Lee et al. (2023).

### 3.2 Framework for network seismic fragility analysis

On top of estimating the network failure probability for one earthquake magnitude, the proposed informative network limit-state functions also enable SS to evaluate network fragility curves. In particular, the intermediate failure domains in SS are now redefined as the failure domain under each  $M_w$ , and their probabilities correspond to discretized points on a fragility curve, with the x-axis representing the magnitude and the y-axis describing the network failure probability. To this end, this section introduces the process of configuring the intermediate failure domains and generating the network fragility curve.

#### 3.2.1 Configuration of the intermediate failure domains

Unlike individual structures, lifeline networks are distributed in a large area. Since IMs are measured differently across all sites for the same earthquake, it is considered more appropriate to use  $M_w$  as the x-axis in the network fragility curves. Consider the case where  $M_w$  changes, while the epicenter remains constant. In that case,  $\mathbf{z}$  is represented as a function of  $M_w$ , i.e.,  $\mathbf{z}(M_w)$ . While seismic demands depend on  $M_w$ , seismic capacities as well as the inter- and intra-event residuals remain unaltered regardless of  $M_w$ . In other words, as  $M_w$  varies, the covariance matrix  $\mathbf{R}_{zz} = [\rho_{z_i z_j}]_{N \times N}$  remains constant, and only the mean of  $\mathbf{z}(M_w)$  changes.

Let  $F_k$  be the network failure domain under an earthquake with the  $k^{th}$  moment magnitude  $M_w^k$ , where  $M_w^1 > M_w^2 > \dots > M_w^m$ . Owing to the constant  $\mathbf{R}_{zz}$ , all distributions of  $\mathbf{z}(M_w^k)$  can be matched to that of  $\mathbf{z}(M_w^1)$  by a linear transformation. Note that, unlike the conventional subset simulation where a relaxation parameter can be explicitly introduced to yield  $\{G(\mathbf{z}(M_w^k)) \leq g_k\}$ , the network limit-state function  $G_{OD}$  is nonlinear and a " $g_k$ " term cannot be factorized out of  $G_{OD}(\cdot)$ . Instead, we define  $F_k$  as

$$F_k = \{G_{OD}(\mathbf{z}(M_w^k)) \leq 0\} = \{G_{OD}(\mathbf{z}(M_w^1) + \mathbf{z}(M_w^k) - \mathbf{z}(M_w^1)) \leq 0\}, \quad (9)$$

where  $k = 1, 2, \dots, m$ . Here, we enforce a constant magnitude decrement, i.e.,  $\Delta M_w = M_w^{k+1} - M_w^k$  is set to a negative constant. Then, Eq. (9) presents an interpretable form of the intermediate failure domains for a

“specialized” SS for the network fragility, an extension of the conventional SS with a relaxation parameter introduced into the limit-state function.

### 3.2.2 Generation of network fragility curves

Using Eq. (9), a single implementation of the specialized SS can yield the network failure probabilities at multiple values of  $M_w$ , i.e., the fragility curve. This practice requires significantly fewer samples than the crude MCS or repeatedly applying SS for each  $M_w$ . If a conditional probability  $P(\mathcal{F}_i|\mathcal{F}_{i-1})$  for a pre-specified magnitude decrement is too small, similar to the conventional SS, we can adaptively reduce the decrement of  $M_w$  so that the conditional probability becomes large, i.e., building an adaptive mesh refinement for the fragility curve.

## 4 Numerical example

One numerical example is considered to demonstrate the efficiency and accuracy of the proposed network limit-state function and the method for network fragility evaluation: two-terminal reliability analysis on a hypothetical network in Figure 1. In each of these examples, the seismic capacity parameters for the components or bridges are fixed at 0.98 for the median  $\bar{C}_i$ , and 0.69 for the log-standard deviation  $\zeta_i$ . To compare the proposed method with the crude MCS, the parameters for HMC-SS are set to  $n = 1,000$ ,  $p_0 = 0.1$ ,  $t_f = \pi/4$ , and  $\alpha = 0$  (for details on the last two parameters, see Wang et al. (2019)). All computations in this section are performed using MATLAB® on an 8-core MacBook Air (2022) with 8 GB of RAM.

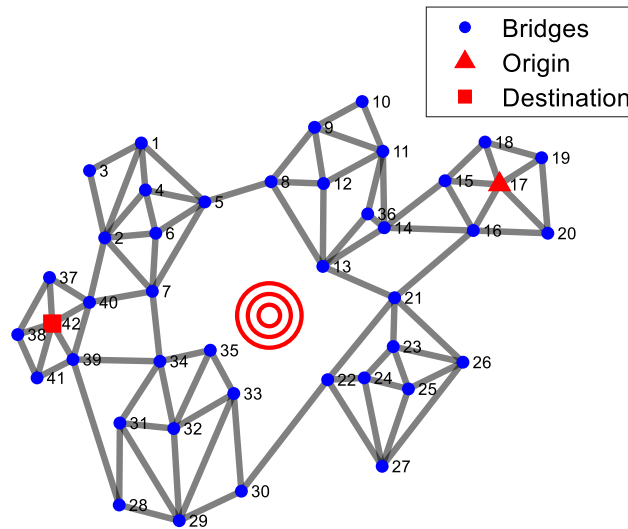


Figure 1. Hypothetical network (Lee & Song 2021).

Consider the hypothetical network in Figure 1 with 42 bridges. To analyze the two-terminal reliability, the HMC-SS using  $G_{OD}^{Pro}$  is conducted 500 times. Two kinds of paths are tested and compared with each other: (1) the most reliable path,  $G_{OD}^{RP}$ , and (2) the shortest path,  $G_{OD}^{SP}$ . The reference MCS solution is obtained through crude MCS with 1% coefficient of variation (*c. o. v.*). Table 1 confirms the accuracy of the HMC-SS using the proposed network limit-state functions; regardless of the used functions, the proposed method shows the high accuracy compared to the MCS results.

Table 1. Two-terminal reliability analysis results for the hypothetical network.

$M_w$	$G_{OD}^{RP}$	$G_{OD}^{SP}$	MCS $P_f$
7.0	$5.14 \times 10^{-2}$	$5.15 \times 10^{-2}$	$5.08 \times 10^{-2}$
6.0	$1.39 \times 10^{-2}$	$1.41 \times 10^{-2}$	$1.37 \times 10^{-2}$
5.0	$2.99 \times 10^{-3}$	$3.01 \times 10^{-3}$	$3.02 \times 10^{-3}$
4.0	$5.46 \times 10^{-4}$	$5.26 \times 10^{-4}$	$5.39 \times 10^{-4}$
3.0	$7.94 \times 10^{-5}$	$7.48 \times 10^{-5}$	$7.92 \times 10^{-5}$

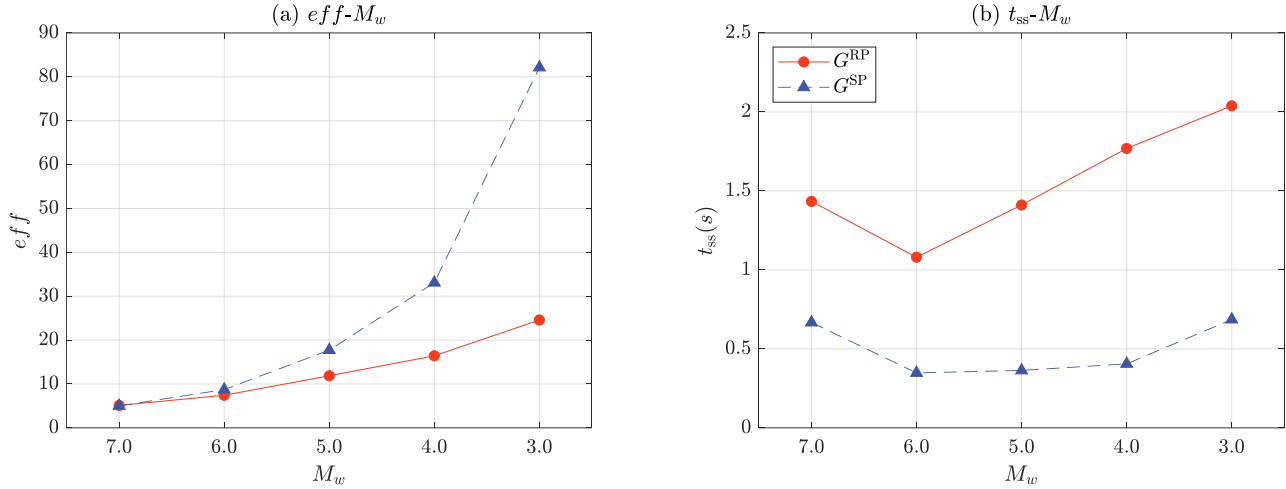


Figure 2. (a)  $eff-M_w$ ; and (b)  $t_{ss}-M_w$  curves on hypothetical network.

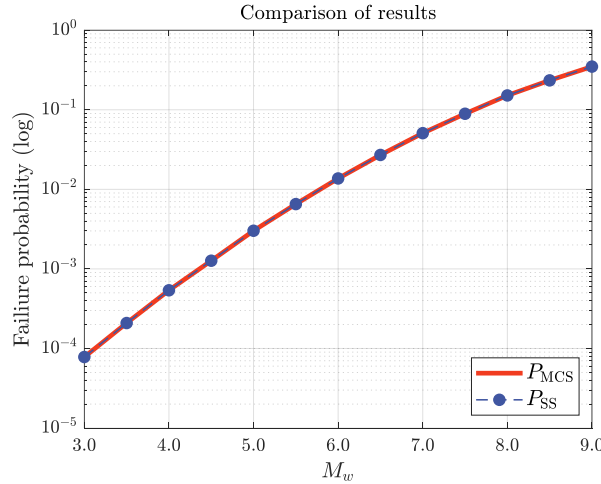


Figure 3. Seismic network fragility curves obtained by a single implementation of specialized HMC-SS.

Figures 2(a) and 2(b) compare the efficiency of the proposed network limit-state functions in terms of  $eff = c.o.v. \times \sqrt{N_G}$ , where  $N_G$  represents the number of limit-state function evaluations; and the computation time  $t_{ss}$  while varying  $M_w$ .  $G_{OD}^{RP}$ -based HMC-SS is more accurate owing to low  $c.o.v.$  of the estimated probabilities, whereas  $G_{OD}^{SP}$ -based HMC-SS takes a much shorter time. The speedup comes from the efficient shortest path search using BFS, which is considerably faster than the Dijkstra algorithm. In general, regardless of the limit-state function, as  $M_w$  decreases, the network failure probabilities decrease, and  $N_G$  and  $t_{ss}$  increase. Then, we evaluate the seismic fragility curve using the framework proposed in Section 3.2. In a single implementation of the specialized HMC-SS,  $G_{OD}^{RP}$  is adopted for its high accuracy, even though it takes longer computation time than using  $G_{OD}^{SP}$ . The range of  $M_w$  is set to  $3.0 \leq M_w \leq 9.0$  with  $\Delta M_w = 0.5$ , and the specialized HMC-SS is repeated 250 times to produce an estimate of the confidence interval. Figure 3 shows the generated seismic fragility curve, compared to the MCS results. The specialized HMC-SS estimates the fragility curve accurately using 11,800 limit-state function evaluations, which is only 38.06% of those required in a repeated simulation of HMC-SS for each  $M_w$ .

## 5 Conclusions

In this study, informative piecewise continuous limit-state functions are proposed for two-terminal reliability analysis of lifeline networks, thus enabling the application of SS. The first limit-state function quantifies the vulnerability of the most reliable path between the origin and destination nodes, while the other uses the shortest path. In addition, a specialized SS is developed to generate network-level fragility curves by

connecting intermediate failure events to the earthquake magnitude. As a result, a single run of the specialized SS can generate the network fragility curve. Future studies can extend the proposed framework to evaluate more realistic network reliability, such as network flow capacity.

## 6 References

- Au S.K., Beck J.L. (2001). Estimation of small failure probabilities in high dimensions by subset simulation. *Probabilistic Engineering Mechanics*, 16(4): 263–277.
- Der Kiureghian A. (2022). *Structural and system reliability*. Cambridge, UK: Cambridge University Press.
- Lee D., Song J. (2021). Multi-scale seismic reliability assessment of networks by centrality-based selective recursive decomposition algorithm. *Earthquake Engineering and Structural Dynamics*, 50(8): 2174–2194.
- Lee, D., Wang, Z., Song, J. (2023). Efficient seismic reliability and fragility analysis of lifeline networks using subset simulation. *arXiv preprint arXiv:2310.10232*.
- Rosenthal A. (1977). Computing the Reliability of Complex Networks. *SIAM Journal on Applied Mathematics*, 32(2): 384–393.
- Wang Z., Broccardo M., Song J. (2019). Hamiltonian Monte Carlo methods for Subset Simulation in reliability analysis. *Structural Safety*, 76: 51–67.